

uBot-7: A Dynamically Balancing Mobile Manipulator with Series Elastic Actuators

Dirk Ruiken¹, Jonathan P. Cummings², Uday R. Savaria¹, Frank C. Sup IV², and Roderic A. Grupen¹

Abstract—We present the next generation of the uBot series: the uBot-7 mobile manipulator with 14 degrees of freedom, 95 cm tall, weighing about 27 kg. The robot is a new, unique mobile manipulator with great versatility to solve tasks in mobility and manipulation. The design is based on experiences from previous uBot generations. We detail the mechanical and electrical layout and highlight the improvements with regards to its predecessor uBot-6. All arm and torso joints are driven by series elastic actuators (SEAs) for better sensing and safer interaction around humans. This makes it the first wheeled dynamic balancer with SEAs. Upgrades to stronger brushless DC motors improve the strength of the robot more than twofold. The head has been extended with two additional motors and now offers independent viewpoint control of the RGB-D camera for all postural configurations of the robot. Finally, a new drive train removes backlash from the base wheels while providing more torque and speed. The design of the robot will be released as open-source.

I. INTRODUCTION AND RELATED WORK

Mobile manipulators are increasingly expected to work in human environments. Research in this area is often conducted with statically stable wheeled robots, such as PR2 and ARMAR-III, that have upper bodies equipped with arms and grippers to interact with the environment [1, 2]. These robots can access most human environments that are wheelchair accessible, but they rely on heavy bases with large footprints to ensure static stability even when reaching for objects far away from the body and when maneuvering at moderate to high speeds.

Dynamically stable robots constantly balance to maintain stability, but require a much smaller footprint and support easier movement in cluttered environments and crowds. Legged humanoids, such as Asimo and ARMAR-4, fall into this category even though they can be statically stable at times [3, 4]. To avoid the complexity of legs on the mechanism in design and control, robots such as the uBot series, Ballbot, and Golem Krang balance on two wheels or a ball to maintain dynamic stability [5–9]. The use of wheels is also much more energetically efficient than the use of legs as the own weight does not have to be carried, and balancing requires very little energy [7]. Additionally, dynamic stability can improve performance in tasks like pushing and lifting as

the body mass can be used more effectively [5, 10, 11]. This, however, comes at the cost of having to prevent or control possible falls.

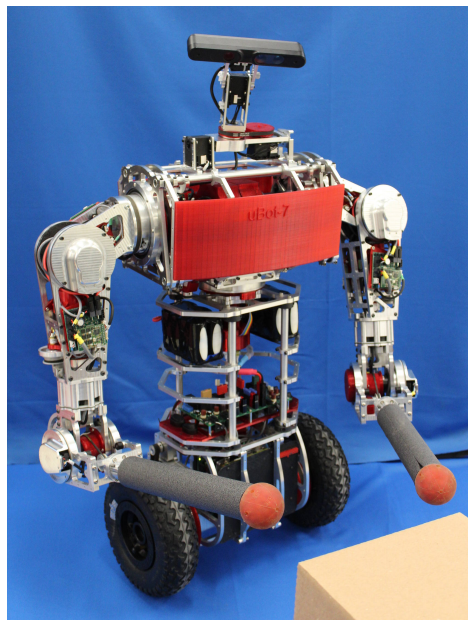


Fig. 1. The uBot-7 mobile manipulator: a dynamically stable robot with 14 active degrees of freedom, 10 series-elastic joints, 27 kg and 95 cm.

The uBot series has been developed as a unique design point combining many advantageous properties into a single robot platform: the uBots have been designed to be large and strong enough to manipulate objects in the real world, yet be small and lightweight enough to be operated easily without complex safety harnesses. At toddler size, the arms can reach table-tops as well as the ground. The small size also makes the robot less intimidating and keeps cost low. Dynamic balancing on two wheels is used to combine great energy efficiency and a small footprint with reduced mechanical and control complexity. Balancing also provides low input impedance longitudinally, making it a good design consideration for safety. Stiff platform impedance laterally supports high manual precision within the bimanual workspace of the robot. Its design avoids highly expensive components, such as harmonic drive gears, in order to keep the robot low cost (for a robot with comparable capabilities) while achieving good performance for manipulation and locomotion.

Based on the concept of having ‘many solutions for many problems,’ the uBot series is a mechanical commitment to solving problems in unstructured environments. For example,

¹Dirk Ruiken, Uday Savaria, and Roderic A. Grupen are affiliated with the Laboratory for Perceptual Robotics, College of Information and Computer Sciences, University of Massachusetts Amherst, USA, ruiken@cs.umass.edu, udaysavaria@gmail.com, grupen@cs.umass.edu

²Jonathan P. Cummings and Frank C. Sup IV are affiliated with the Department of Mechanical and Industrial Engineering, University of Massachusetts Amherst, USA, cummi3@gmail.com, sup@umass.edu

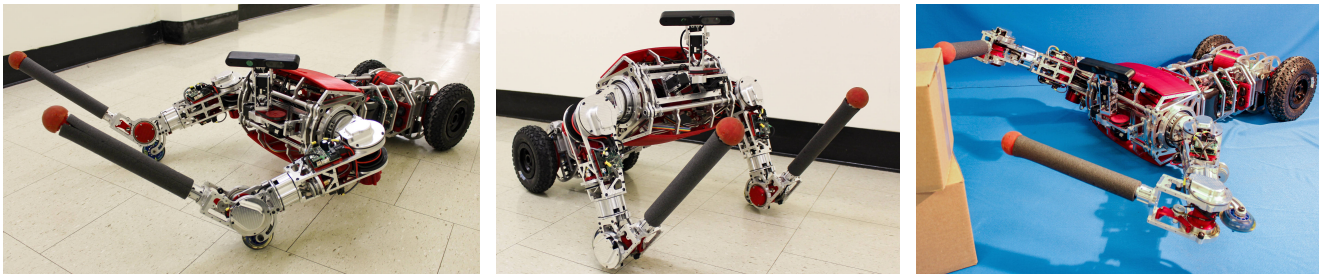


Fig. 2. Examples of three statically stable postural configurations of uBot-7: four point contact with elbow and base wheels at low body height (left) and high body height (middle) support alternative forms of mobility with reduced manipulation capabilities; lying prone provides maximal stability and leaves the arms free for manipulation (right).

uBot-6 added different postural configurations [7]. Each configuration supports different properties to both manipulation and mobility (Fig. 3). Transitioning to a statically stable configuration can greatly increase manual precision and enable successful completion of otherwise impossible tasks. Likewise, different postural configurations also support different forms of mobility that can help overcome obstacles in the environment and make areas without smooth flat ground accessible [12]. The previous two models of the uBot series, uBot-5 and uBot-6, have been used successfully in many applications ranging from object recognition/manipulation [13], autonomous assembly [14, 15], emergency response [16], and physical rehabilitation [17, 18].

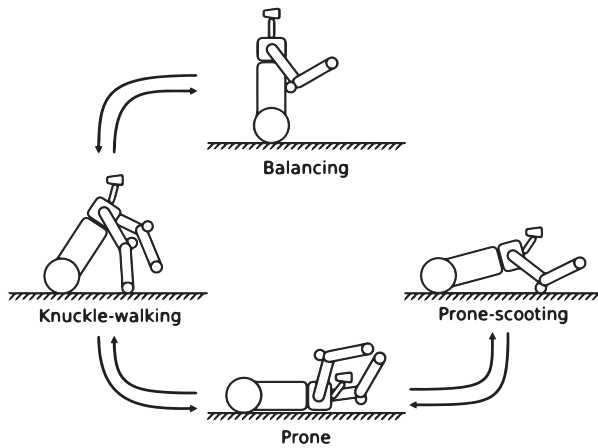


Fig. 3. Transitions between postural configurations and the respective modes of mobility. Balancing is highly energy efficient, but requires a relatively flat ground. Knuckle-walking enables traversing rough terrain by using the arm for walking. Prone-scooting supports statically stable mobility at a lower body height by using passive wheels on the elbows.

With advances in mobile manipulation, interest is increasing in robots working side by side with humans. Safety is the main concern in such scenarios. Accidental impacts with humans should have minimal potential of injuring them and need to be detected by the robot. The most popular method to implement this functionality in robots is the use of impedance control [19]. This can either be done on robots with series elastic actuators (SEAs) [20] with passive compliance at the expense of precision, for example Baxter and COMAN [21, 22], or on robots with high performance torque

sensing capabilities, for example DLR's Justin [23, 24].

uBot-7 (Fig. 1) has been developed to incorporate SEAs into a versatile platform such as predecessor uBot-6. It is a toddler-sized mobile manipulator with 14 degrees of freedom (DOF). It has two 4-DOF arms, a rotatable trunk, and a 3-DOF head. The robot weighs about 27 kg and is 95 cm tall. In its primary form of locomotion the robot is a dynamic balancer on two wheels. The wheels provide non-holonomic drive capabilities with differential steering. Just like uBot-6, it is capable of transitioning to and between other postural configurations (Fig. 2) [7]. Each postural configuration enables additional ways to interact with the environment and solve tasks. At the same time they also pose additional requirements to the robot design. A new improved head mechanism accommodates many of these requirements in order to extend the capabilities to interact with the environment and solve tasks in any postural configuration. The addition of SEAs to all arms and torso joints extends the passive, anisotropic impedance character of its base into an active impedance character in the upper body.

The experience with predecessor uBot-6 resulted in two architectural changes:

- All arm and torso joints are driven by SEAs that support impedance control for safer operation near humans. The SEAs also provide force/torque sensing for better manipulation capabilities. Additionally, the passive properties of SEAs combined with reactive control can protect gearheads from damage in case of a fall. A modular SEA module was developed for uBot-7 [25–27].
- The head has been extended with two more active degrees of freedom to support full pan-tilt view of the entire robot workspace that is independent of the postural configuration. Previously, this capability was only available while balancing and required the use of the trunk rotation.

A number of smaller improvements include:

- Motors were switched from brushed DC to brushless DC (BLDC) motors resulting in about twofold increase in strength.
- Backlash in the wheel drive train can cause problems while balancing. An improved drive train eliminates backlash while increasing wheel torque and speed.
- The control architecture was switched to a decentralized strategy, removing harness complexity, alleviating

difficulty of cable routing, and reducing possible failure points (connectors).

The main contribution of this paper is the presentation of the complete design of the new, unique mobile manipulator, uBot-7. The base structure and the SEA modules have been previously documented [25, 26]. This paper presents the fully integrated robot platform with embedded systems, sensors, and control architecture. To our knowledge it is the first dynamically balancing wheeled mobile manipulator with SEAs. Its design has been evolved over many robot generations to combine many advantages from different areas into a single platform. It offers a unique versatility to solve tasks in mobility and manipulation while being low cost and easy to operate. The design of uBot-7 will be made open-source and available on <http://lpr.cs.umass.edu/ubot> in hopes to enable other researchers with the capabilities of this platform.

The mechatronic design of uBot-7 will be presented in Section II. Emphasis is given to details that have been improved from previous models. Section III describes the motor control system, sensors, the available computing hardware, and the interprocess communication architecture. We conclude in Section IV and outline future work.

II. MECHATRONIC DESIGN

The mechanical design can be separated into three different parts: the head, arms and torso, and the wheeled base. In the following sections, we present details of each part, highlighting the improvements based on experiences from work with uBot-4/5/6 [5–7, 27].

A. Head

The head design is based on experiences from uBot-6 [7]. The head of uBot-6 uses two coupled joints driven by a single actuator to enable compensation of different body angles due to dynamic balancing as well as different postural modes (Fig. 4). Panning capabilities could be performed by rotating the torso though this is only available while balancing upright. Additionally, it enables moving the camera forward to provide an unobstructed view of the space in front of the robot.

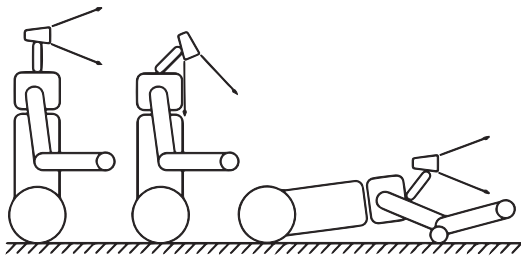


Fig. 4. Examples of different requirements for camera direction: upright balancing (left), unobstructed view of the manual workspace (middle), four-point contact postural configuration for prone scooting (right) [7].

The head for uBot-7 keeps these capabilities, but enables head panning and tilting independently of the torso rotation joint. It uses three active degrees of freedom: a tilt joint at the

base followed by a pan and a tilt joint on top (Fig. 5). The lower tilt joint matches the capabilities introduced in uBot-6. The pan-tilt unit on top adds the much needed capability to point the camera independently of the postural configuration and body angle. All head joints are based on Dynamixel MX-28 servos with integrated sensors. Joint characteristics can be found in Table I.

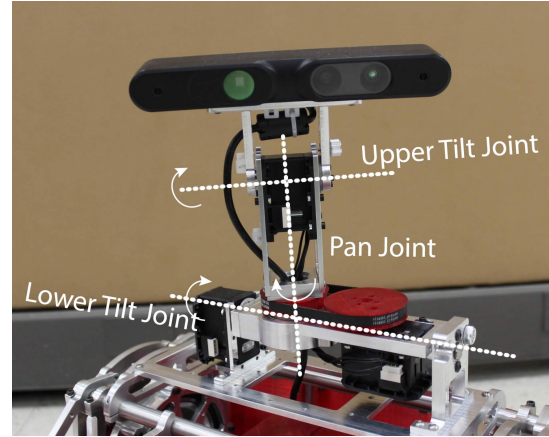


Fig. 5. uBot-7 head with three active degrees of freedom: tilt, pan, tilt. The first tilt joint supports compensation of body angle of the dynamic balancer and enables pan-tilt motion in all postural modes. Axes of rotation for each joint are shown in white.

B. Arms and Torso

Each arm consists of four degrees of freedom: shoulder flexion, shoulder abduction, shoulder twist, and an elbow with a passive wheel for prone scooting. The two arms provide a large bimanual workspace that is symmetric in the front and back of the robot and includes much of the ground plane (Fig. 6). The joint for trunk rotation extends the bimanual workspace all around the robot.

Each arm and torso joint is driven by an SEA. In order to simplify incorporation of SEAs in several joints, we developed a modular package that can be customized to the various requirements of different joints [25]. Figure 9 shows

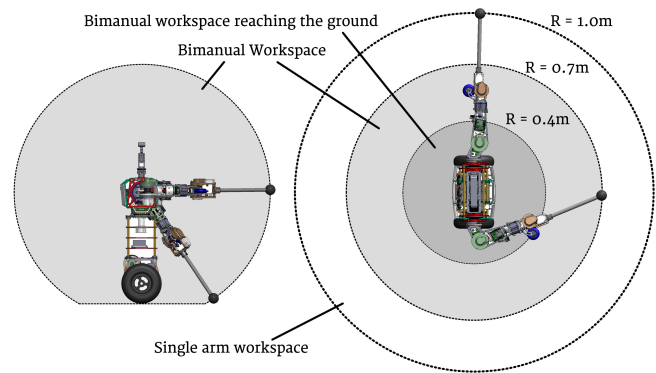


Fig. 6. Workspace of uBot-7: Single arm workspace, bimanual workspace, and bimanual workspace on the ground. When only the arm joints are used, some locations close to the robot body cannot be reached due to self collisions. But the use of the rotatable trunk makes these locations reachable, and each workspace extends completely around the robot.

TABLE I
JOINT CHARACTERISTICS FOR uBOT-6 AND uBOT-7

		Continuous torque [Nm]		Max. angular speed [deg/s]		Range of Motion [deg]	Motors uBot-7
		uBot-6	uBot-7	uBot-6	uBot-7		
Head	Upper Tilt	–	0.6	–	400	[-90, 90]	Dynamixel MX-28
	Pan	–	0.6	–	400	[-200, 200]	Dynamixel MX-28
	Lower Tilt	0.6	0.6	850	400	[-90, 90]	Dynamixel MX-28
Torso		2.6	12.0	570	234	[-165, 165]	Maxon ECflat 45 (70W)
	Shoulder	15.0	45.0	100	114	[-360, 360]	Maxon ECflat 90 (90W)
	Roll	6.4	21.0	237	162	[-30, 180]	Maxon ECflat 45 (70W)
	Pitch	6.4	12.0	237	234	[-80, 260]	Maxon ECflat 45 (70W)
	Yaw	6.4	12.0	237	234	[-60, 100]	Maxon ECflat 45 (70W)
Elbow		2.4	4.2	900	1900	continuous	Maxon ECflat 90 (90W)
Wheel							

the different arm joints equipped with the modular SEAs. Figure 7 shows a detailed view of the modular SEA in the shoulder abduction joint. Each SEA module combines flat brushless DC (BLDC) motors, planetary gearheads, and flat torsional spring designs in order to remain lightweight, low-volume, easy to reconfigure, and high performing. The spring design (Fig. 8) has a linear torque-displacement relationship. It was developed in collaboration with partners at the Johnson Space Center and is similar to the spring design used in NASA’s Robonaut 2 [28, 29].

Absolute position sensors measure the position of the joint output at high resolution. Joint torque is determined by measuring the deflection of the torsional spring directly with a Hall effect sensor providing an extremely cheap sensor with decent resolution (see [25] for a detailed discussion).

All components of the SEA module (except the springs) are commercially available and affordable enough to match the low-cost principle of the uBot series. The spring design is based on two-dimensional cutting operations and can be machined easily.

The experiences with uBot-5 and uBot-6 were used to select appropriate joint torques, velocities, and ranges of motion (see Table I). The velocity requirements are based on the need to execute bracing actions in case of a potential fall. As the robot can knuckle-walk with its arms, it needs to be strong enough to support its body weight. The range of motions were chosen to provide the large bimanual workspace all around the robot.

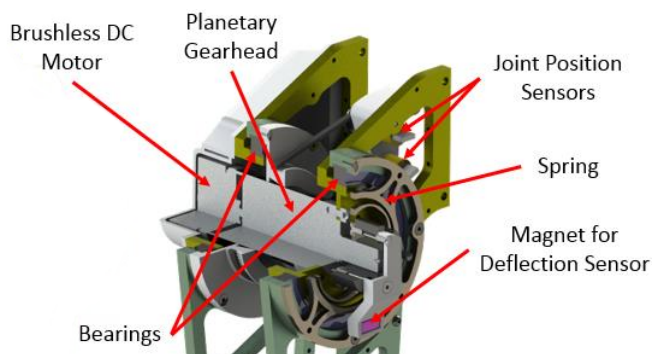


Fig. 7. Components of the SEA for shoulder abduction. The motor/gearhead output shaft is connected to the center of a torsional spring and the outside of the spring is connected to the link of the joint. A Hall effect sensor measures the displacement of a magnet to measure the spring deflection.

As the uBot can balance on a differentially steered, two-wheeled base and may fall, the resulting loads on the arms may exceed normal design loads. The passive properties of SEAs combined with reactive control can protect gearheads from damage. A larger passive compliance is desired to provide enough reaction time for actively moving joints out of the way and gracefully absorbing impacts once an impact is detected. A larger maximum spring deflection also improves the sensing resolution, but makes precise control more difficult. Therefore, we chose a maximum spring deflection of ± 4 deg as a trade-off between manual precision and torque sensing resolution. The spring constants for each joint were chosen based on maximum joint torque and the maximum spring deflection. This results in sensing resolutions between 0.011 Nm (elbow) and 0.044 Nm (shoulder). The spring constant of the used springs is linear in the thickness of the spring. Thus the spring constants can easily be changed by installing thicker or thinner springs.

C. Drive System

The main drawback of the uBot-6 drive system has been the presence of backlash in the gearheads of the drive motors. As balancing requires frequent direction changes just at the equilibrium point, this backlash can be very noticeable. With every direction change, the gear first moves through the backlash region before providing torque in the other direction. As a result, wheel chattering can occur when standing still and only small wheel corrections are required.

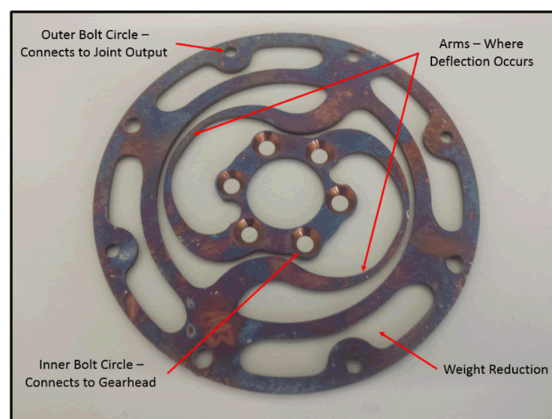


Fig. 8. Torsional spring design with a linear torque-displacement relationship used in the modular SEAs.

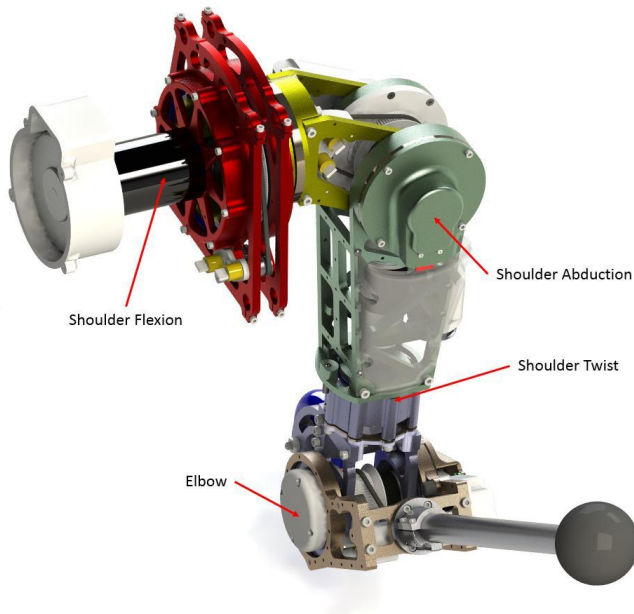


Fig. 9. Rendering of an arm consisting of four four joints equipped with SEAs.

This issue has been addressed in a new drive train design for uBot-7. Powerful 90 W flat BLDC motors provide much higher torque to the drive wheels and thus only a very small additional gear reduction is needed. We use timing belts to provide a backlash-free 7.5:1 gear reduction to the wheels. The change roughly doubles available continuous torque, maximum torque, and maximum velocity while removing backlash issues. A special embedded control board (Section III-A) was designed to handle control of both wheel motors as well as measurements from inertial measurement units (IMUs) to ensure all resources required for balancing are in one place.

III. CONTROL ARCHITECTURE

uBot-6 employs a centralized motor control strategy and controls all joints from a single field programmable gate array (FPGA). On uBot-7, motor controllers are distributed over the whole robot and placed close to the respective joints. Sensors and motors are interfaced locally, and only a communication bus and power need to be routed. As a result only a small number of cables run through the arms, simplifying routing. The freed space in the torso can house additional on-board computing hardware. Up to six lithium iron phosphate (LiFePO_4) battery packs can be housed in the trunk of the robot. The operation time of the robot on these batteries has not been tested yet, but uBot-6 could operate about one hour on two battery packs. It is important to note that the power consumption is heavily dominated by the on-board computer. Under full processing load the computer needs 45 W while the remainder of the robot only consumes 2.6 W while just balancing.

A. Motor Control System

The arms, torso, and wheels are driven by brushless DC motors (BLDC). Custom embedded controller boards for mo-

tor control and sensor processing are distributed throughout the body in proximity of the respective joints. The custom PCBs are built around Maxon ESCON 50/5 motor control modules. A PIC32MX 80 MHz microcontroller interfaces the motor control modules, sensors, and the communication bus. It currently supports position, velocity, torque, and impedance control at 1 KHz control rate and allows full access to extend the programming.

We designed two different custom controller boards that are able to control one or two joints: All arm joints as well as the torso joint are each equipped with a single embedded controller board per joint. Both wheel motors share a single controller board with two motor driver modules. This controller board also directly interfaces two inertial measurement units (IMUs). By combining all sensor input, computation, and motor control needed for balancing on a single embedded controller board, balancing control becomes independent of possible problems with the control computer or board-to-board communication. The control computer calculates shifts in the center of mass of the robot based on all joint angles and passes them as parameters to the balancer running on the embedded hardware.

B. Sensors

The robot is equipped with a wide range of sensors (Table II). All arm and torso joints are driven by SEAs. Each uses a Hall effect sensor to determine joint torque by measuring the deflection of the torsional spring. Joint output positions are measured with absolute position sensors at high resolution (10-13 bpr). Several joints have a larger range of motion than could be handled by a single absolute position sensor at the desired resolution. Therefore, two absolute position sensors are combined with two different gear reductions. The phase difference between the sensor signals supports calculation of a high resolution absolute position over the whole range of motion. The same method also enables acquiring a high resolution measurement from two (cheaper) low resolution sensors [25]. The wheel motors are not driven by SEAs, and an incremental position encoder at the motor provides sufficient feedback. Both wheels are controlled by a single microcontroller that uses the feedback of an onboard IMU chip to perform balancing control. An additional external IMU placed near the robot's center of mass can be connected directly to provide more robustness to external disturbances and impacts. All embedded controller boards also provide current sensing. The head joints use Dynamixel servo motors that provide feedback of joint positions, velocities, and torques. An Asus Xtion Pro Live mounted on the head delivers RGB-D information at 30 Hz [30]. In the future, both arms will be equipped with 6-DOF force/torque sensors.

C. PC System

The robot is equipped with two on-board computers. An embedded pico-ITX computer with a quad-core 6th generation 2.6 GHz Intel Core-i7 processor is housed in the base of the robot. It handles communication with the distributed

TABLE II
SENSORS OF uBOT-7

Sensor	Type	Manufacturer	Position	Quantity
IMU	BM055	Bosch	Base, Torso	2
Absolute encoders	MA3	US Digital	Arms, torso	14
Incremental encoders	MILE	Maxon	Wheel motors	2
Current sensing	Escon 50/5	Maxon	Arms, torso, wheels	11
Torque sensor	90363	Melexis	Arms, torso,	9
Position sensor	MX-28	Dynamixel	Head	3
6 DOF force/torque	Mini45	ATI	Wrists	2
Camera/RGB-D	Xtion Pro Live	Asus	Head	1

motor controller and sensor boards and any Cartesian control. Additionally, it can perform high-level planning and control. A Jetson TX1 board adds capabilities for GPU accelerated processing for applications like vision, planning, and deep learning [31, 32]. Additional space is available to add more compute hardware to the robot in the future.

D. Communication

An overview of the compute and communication architecture used on uBot-7 is shown in Figure 10. The on-board computers communicate over Gigabit Ethernet. A mini-router provides reliable WiFi connectivity for all on-board computers with the ability to secure all off-board communication through a virtual private network (VPN).

The distributed motor controllers for wheels, arms, and torso are connected to the control computer through a RS-485 communication bus running at 10 Mbps which is fast enough to support real-time control. The head motors are connected through another RS-485 bus running at 2 Mbps.

The ASUS Xtion Pro Live sensor is connected through USB to the vision computer. A software interface exists for the robot operating system (ROS) that supports interfacing to all joints and sensors of the robot for easy application development [33]. The interface is compatible with previous uBot versions and existing applications will transfer to the new robot with minimal changes.

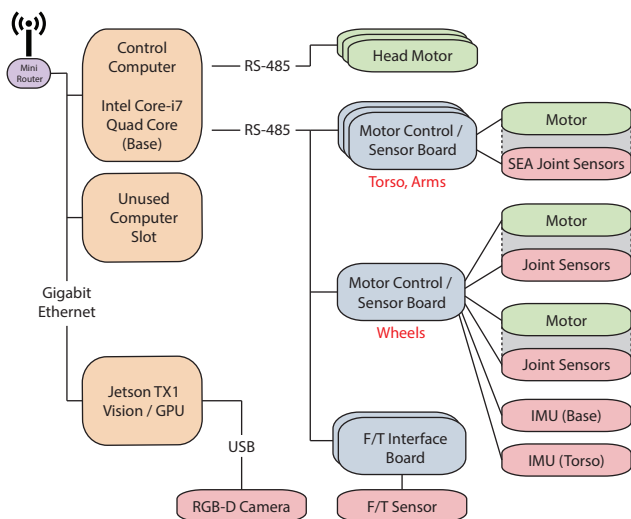


Fig. 10. Computer and communication architecture of uBot-7.

IV. CONCLUSION AND FUTURE WORK

We presented uBot-7, the newest member of the uBot series of mobile manipulators. To our knowledge, this is the first wheeled dynamic balancer with series elastic actuators (SEAs). The SEAs will provide increased performance for manipulation tasks, safety mechanisms for the robot in case of falls, and the ability to detect accidental collisions to work around humans more safely. The capability of changing postural configurations and mobility modes enables operation outside of areas with flat and smooth floors. Added degrees of freedom in the head support much better perceptual performance that is independent of these postural configurations. The overall design of uBot-7 adds great versatility to solve tasks in manipulation and mobility over its predecessor uBot-6. The design of uBot-7 will be open-source and available at <http://lpr.cs.umass.edu/ubot> in hopes to enable other researchers with the capabilities of this platform.

Implementation and tests of the low-level control have been completed, and full operation is expected soon. Future work will focus on transferring existing capabilities for dexterous manipulation and mobility from uBot-6. Additionally, we will focus on investigating better manipulation strategies based on the improved control and sensing capabilities. Several hands have already been prototyped that could increase the capabilities for manual interaction while being capable of supporting the weight of the robot during knuckle-walking without damaging hands or fingers.

ACKNOWLEDGMENT

We thank Oliver Fyler for his work on the head prototype. This material is based upon work supported under Grant NASA-GCT-NNX12AR16A. Any opinions, findings, conclusions, or recommendations expressed in this material are solely those of the authors and do not necessarily reflect the views of the National Aeronautics and Space Administration.

REFERENCES

- [1] J. Bohren, R. B. Rusu, E. G. Jones, E. Marder-Eppstein, C. Pantofaru, M. Wise, L. Mösenlechner, W. Meeussen, and S. Holzer, "Towards autonomous robotic butlers: Lessons learned with the PR2," in *2011 IEEE International Conference on Robotics and Automation (ICRA)*. IEEE, 2011, pp. 5568–5575.
- [2] T. Asfour, K. Regenstein, P. Azad, J. Schröder, and R. Dillmann, "ARMAR-III: A humanoid platform for perception-action integration," in *Proc., International Workshop on*

- Human-Centered Robotic Systems (HCRS), Munich*. Citeseer, 2006, pp. 51–56.
- [3] Y. Sakagami, R. Watanabe, C. Aoyama, S. Matsunaga, N. Higaki, and K. Fujimura, “The intelligent ASIMO: System overview and integration,” in *IEEE/RSJ International Conference on Intelligent Robots and Systems, 2002.*, vol. 3. IEEE, 2002, pp. 2478–2483.
 - [4] T. Asfour, J. Schill, H. Peters, C. Klas, J. Bücken, C. Sander, S. Schulz, A. Kargov, T. Werner, and V. Bartenbach, “ARMAR-4: A 63 DOF torque controlled humanoid robot,” in *2013 13th IEEE-RAS International Conference on Humanoid Robots (Humanoids)*. IEEE, 2013, pp. 390–396.
 - [5] P. Deegan, B. J. Thibodeau, and R. Grupen, “Designing a self-stabilizing robot for dynamic mobile manipulation,” DTIC Document, Tech. Rep., 2006.
 - [6] S. Kuindersma, E. Hannigan, D. Ruiken, and R. Grupen, “Dexterous mobility with the uBot-5 mobile manipulator,” in *International Conference on Advanced Robotics 2009 (ICAR)*, 2009, pp. 1–7.
 - [7] D. Ruiken, M. W. Lanighan, and R. A. Grupen, “Postural modes and control for dexterous mobile manipulation: The UMass uBot concept,” in *Proc. of IEEE-RAS Int. Conf. on Humanoid Robots (Humanoids)*, 2013.
 - [8] T. Lauwers, G. A. Kantor, and R. Hollis, “A dynamically stable single-wheeled mobile robot with inverse mouse-ball drive,” in *Robotics and Automation, 2006. ICRA 2006. Proceedings 2006 IEEE International Conference on*. IEEE, 2006, pp. 2884–2889.
 - [9] M. Stilman, J. Olson, and W. Gloss, “Golem Krang: Dynamically stable humanoid robot for mobile manipulation,” in *2010 IEEE International Conference on Robotics and Automation (ICRA)*. IEEE, May 2010, pp. 3304–3309.
 - [10] P. Kolhe, N. Dantam, and M. Stilman, “Dynamic pushing strategies for dynamically stable mobile manipulators,” in *2010 IEEE International Conference on Robotics and Automation (ICRA)*. IEEE, 2010, pp. 3745–3750.
 - [11] S. R. Kuindersma, R. A. Grupen, and A. G. Barto, “Variable risk control via stochastic optimization,” *The International Journal of Robotics Research*, vol. 32, no. 7, pp. 806–825, 2013.
 - [12] D. Ruiken, M. W. Lanighan, and R. A. Grupen, “Path planning for dexterous mobility,” in *International Conference on Automated Planning and Scheduling (ICAPS)*, 2014.
 - [13] D. Ruiken, J. M. Wong, T. Q. Liu, M. Hebert, T. Takahashi, M. W. Lanighan, and R. A. Grupen, “Affordance-based active belief: Recognition using visual and manual actions,” in *2016 IEEE/RSJ International Conference on Intelligent Robots and Systems (IROS)*. IEEE, 2016, pp. 5312–5317.
 - [14] D. Ruiken, T. Q. Liu, T. Takahashi, and R. A. Grupen, “Reconfigurable tasks in belief-space planning,” in *2016 IEEE-RAS 16th International Conference on Humanoid Robots (Humanoids)*. IEEE, 2016, pp. 1257–1263.
 - [15] R. A. Grupen, M. W. Lanighan, and T. Takahashi, “Hybrid task planning grounded in belief: Constructing physical copies of simple structures,” in *International Conference on Automated Planning and Scheduling (ICAPS)*, 2017.
 - [16] H.-T. Jung, T. Takahashi, and R. Grupen, “Human-robot emergency response-experimental platform and preliminary dataset,” DTIC Document, Tech. Rep., 2014.
 - [17] H.-T. Jung, J. Baird, Y.-K. Choe, and R. A. Grupen, “Upper extremity physical therapy for stroke patients using a general purpose robot,” in *RO-MAN, 2011 IEEE*. IEEE, 2011, pp. 270–275.
 - [18] H.-T. Jung, T. Takahashi, Y.-K. Choe, J. Baird, T. Foster, and R. A. Grupen, “Towards extended virtual presence of the therapist in stroke rehabilitation,” in *2013 IEEE International Conference on Rehabilitation Robotics (ICORR)*. IEEE, 2013, pp. 1–6.
 - [19] N. Hogan, “Impedance control - An approach to manipulation. I - Theory. II - Implementation. III - Applications,” *ASME Transactions Journal of Dynamic Systems and Measurement Control B*, vol. 107, pp. 1–24, Mar. 1985.
 - [20] G. A. Pratt and M. M. Williamson, “Series elastic actuators,” in *Proceedings. 1995 IEEE/RSJ International Conference on Intelligent Robots and Systems 95: Human Robot Interaction and Cooperative Robots*, vol. 1. IEEE, 1995, pp. 399–406.
 - [21] R. Robotics. (2017) Baxter Collaborative Robots for Industrial Automation. [Online]. Available: <http://www.rethinkrobotics.com/baxter/>
 - [22] N. G. Tsagarakis, S. Morfey, G. M. Cerda, L. Zhibin, and D. G. Caldwell, “Compliant humanoid COMAN: Optimal joint stiffness tuning for modal frequency control,” in *2013 IEEE International Conference on Robotics and Automation (ICRA)*. IEEE, 2013, pp. 673–678.
 - [23] C. Ott, O. Eiberger, W. Friedl, B. Bauml, U. Hillenbrand, C. Borst, A. Albu-Schaffer, B. Brunner, H. Hirschmuller, S. Kielhofer, et al., “A humanoid two-arm system for dexterous manipulation,” in *2006 6th IEEE-RAS International Conference on Humanoid Robots*. IEEE, 2006, pp. 276–283.
 - [24] T. Wimbock, C. Ott, and G. Hirzinger, “Impedance behaviors for two-handed manipulation: Design and experiments,” in *2007 IEEE International Conference on Robotics and Automation (ICRA)*. IEEE, 2007, pp. 4182–4189.
 - [25] J. P. Cummings, D. Ruiken, E. L. Wilkinson, M. W. Lanighan, R. A. Grupen, and F. C. Sup, “A compact, modular series elastic actuator,” *Journal of Mechanisms and Robotics*, vol. 8, no. 4, p. 041016, 2016.
 - [26] J. Cummings, “uBot-7: The design of a compliant dexterous mobile manipulator,” Master’s thesis, University of Massachusetts Amherst, 2014.
 - [27] D. Ruiken, “Belief-space planning for resourceful manipulation and mobility,” Ph.D. dissertation, University of Massachusetts Amherst, 2017.
 - [28] M. A. Diftler, J. Mehling, M. E. Abdallah, N. A. Radford, L. B. Bridgwater, A. M. Sanders, R. S. Askew, D. M. Linn, J. D. Yamokoski, F. Permenter, et al., “Robonaut 2-the first humanoid robot in space,” in *2011 IEEE International Conference on Robotics and Automation (ICRA)*. IEEE, 2011, pp. 2178–2183.
 - [29] C. A. Ihrke, J. S. Mehling, A. H. Parsons, B. K. Griffith, N. A. Radford, F. N. Permenter, D. R. Davis, R. O. Ambrose, L. Q. Junkin, et al., “Rotary series elastic actuator,” Oct. 23 2012, US Patent 8,291,788.
 - [30] ASUS. (2017) ASUS Xtion PRO LIVE. [Online]. Available: https://www.asus.com/us/3D-Sensor/Xtion_PRO_LIVE/
 - [31] Nvidia. (2017) Nvidia Jetson TX1 the embedded platform for autonomous everything. [Online]. Available: <http://www.nvidia.com/object/jetson-tx1-module.html>
 - [32] K. H. Wray, D. Ruiken, R. A. Grupen, and S. Zilberstein, “Log-space harmonic function path planning,” in *2016 IEEE/RSJ International Conference on Intelligent Robots and Systems (IROS)*. IEEE, 2016, pp. 1511–1516.
 - [33] M. Quigley, K. Conley, B. Gerkey, J. Faust, T. Foote, J. Leibs, R. Wheeler, and A. Y. Ng, “ROS: An open-source robot operating system,” in *ICRA workshop on open source software*, vol. 3, no. 3.2, 2009.